Response and instabilities of the lamellar phase of diblock copolymers under uniaxial stress

Zhen-Gang Wang
Division of Chemistry and Chemical Engineering, California Institute of Technology, Pasadena, California 91125

(Received 16 August 1993; accepted 12 October 1993)

We study the quasistatic behavior of the lamellar phase of diblock copolymers under uniaxial compression and tension along the normal direction of the layers, in both the weak segregation limit (WSL) and the strong segregation limit (SSL). In the SSL, we derive a (nonlinear) continuum free energy description of the system in terms of local displacement of the lamellar layers, and use this free energy to study the mechanical behaviors. While compression induces the usual Hookian elastic response (for strains or stresses that are not too large), tension leads to square-lattice wave undulations in the transverse directions when the strain exceeds a critical value. In the WSL close to the order–disorder transition temperature, compression can "melt" the lamellar phase to the isotropic phase; such a melting can take the form of three types of instabilities, a quasithermodynamic instability, a spinodal at controlled strain, and a mechanical instability at controlled stress. It is shown that the third instability always precedes the second one under controlled-stress conditions. For a weakly first-order transition, the quasithermodynamic instability precedes the mechanical instability; but for a (hypothetical) second-order transition, the mechanical instability appears first as the stress is increased. In the case of tension, a transverse square-lattice wave deformation again develops at a critical strain. This deformation can be followed by a subsequent melting of types similar to the compressional case, upon further increase of the stress or strain. In both the SSL and WSL, the modulus undergoes an abrupt decrease when layer undulation develops, to a value 7/15 of that before the onset of undulation. Because the critical strain for the onset of undulation is usually very small, the modulus for tension will appear different from the modulus for compression, the former being 7/15 of the latter. As a result of this decrease in the modulus, melting of the lamellar phase in the WSL will occur at larger strains under tension than under compression.

I. INTRODUCTION

Complex molecules, molecules having a large number of degrees of freedom and often competing entropic and energetic forces, often form microstructured fluids whose properties are intermediate between those of liquids and solids. On the microscopic level the molecules possess quite a bit of fluidity, lacking any conspicuous order, and yet on a mesoscopic scale, the system can exhibit solidlike, long-range periodic structures. The relaxation time associated with the mesoscopic structural changes are usually much longer than the relaxation time of the molecular segments. Thus, within certain time scales, these ordered fluids can often possess finite, quasistatic elastic moduli with respect to deformation of the structures in one or more directions. Diblock copolymer melts with incompatible blocks provide a good example, where structures ranging from stacked bilayers to hexagonally-packed cylinders to body-centered-cubic-packed globules can be obtained by changing the temperature and/or the composition of the diblocks.[1] Understanding the mechanical behaviors of these structures is both of intellectual interest and of practical importance because many applications of polymeric materials derive from their unique mechanical properties.

In this paper, we study the quasiequilibrium behavior of the simplest of the microstructured diblock copolymer phases, namely that of a single-domain lamellar phase, under uniaxial stress. This phase is obtained when the two incompatible blocks are of approximately equal lengths. Single-domain samples can be obtained, for example, by flow-induced alignment.[2–4] Consider a lamellar phase with the equilibrium layer spacing which is subjected to compressional or tensile strain or stress in the direction normal to the layers. In a full equilibrium state, the system would readjust itself to the newly imposed dimension by changing the number of layers. However, such global structural rearrangements involve the creation and movement of edge dislocations; the time scale for such events for long polymers can be much longer than the typical time scale of the stress or strain experiments. Thus within certain ranges of the time scale, the system can remain in a constrained (metastable) equilibrium state with a *fixed number of layers*. This is in fact the very reason that lamellar phases, or smectic liquid-crystals in general, have well-defined, finite elastic moduli. In order that the responses are quasiequilibrium, however, the time scale of the stress or strain experiments has to be much longer than the typical internal stress relaxation time, but much shorter than the time scale associated with changing the number of layers. This requirement does not seem to be much of a restriction on the applicability of our study; many commercially available copolymers of the Kraton-type, such as polystyrene–polyisoprene, often have blocks whose molecular weights are below or about their respective entanglement molecular

 0021-9606/94/100(3)/2298/12/$6.00

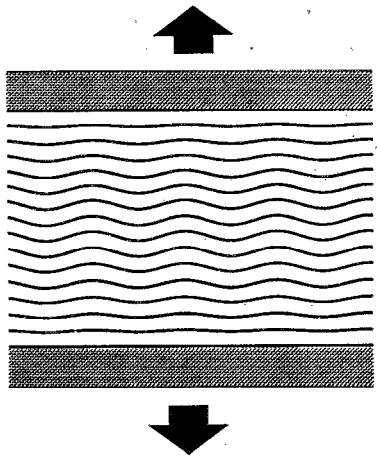

FIG. 1. Schematic cross-sectional view of layer undulation induced by tension. Only the surfaces of the average location of the A–B junction points are shown in this figure; composition variation is not indicated. Also, the actual wave pattern is that of a square-lattice wave; see the text.

weights, and yet microphase-separate above their glass transition temperatures.[5] Even for very long polymers well above the entanglement molecular weight, whose relaxation time for compressional stress in the strong segregation limit increases exponentially with the degree of polymerization,[6] the condition can still be satisfied as the time scale for changing the number of layers is expected to be even longer. In the latter case, however, the time it takes to perform the relevant experiments also becomes long.

Given that the conditions for quasiequilibrium can be achieved, we wish to answer the following questions. How does the system respond to an imposed stress or strain? What is the maximum stress the lamellar phase can sustain? In the strong segregation limit (SSL), the response of the lamellar structure to a compressional strain is expected to be simple (at least for not too large strains); the layer spacing decreases, leading to a free energy cost which is quadratic in the strain; this gives rise to the usual Hookian elasticity. When the system is subjected to a tensile strain, however, the layers have the option to partially relieve the internal stress by buckling, as illustrated in Fig. 1, because the true distance between two adjacent layers undulating in phase is now shorter than the vertical distance. This undulation instability is well-known for smectic-A liquid crystals, and takes place at very small strains under typical experimental situations.[7–10] In the weak segregation limit (WSL), both the layer spacing and the amplitude of the composition waves deviate from the equilibrium values when finite strains are imposed. This can lead to "melting" of the lamellar structure to the isotropic state for large enough strains, because the free energy of the lamellar phase increases with increasing strains while the free energy of the isotropic state is independent of the strain. Under tensile strains, the melting will be preceded by the undulation instability of the layers, similar to the SSL case.

Similar issues have recently been addressed by Amundson and Helfand.[11] These authors focus on the (linear) elastic moduli of the lamellar phase as a function of temperature, the shift of the phase transition temperatures due to an imposed strain, and the free energy cost for creating certain types of defects, all in the WSL. In our study, we focus rather on the behavior of the lamellar phase under uniaxial *stress*. The distinction between the strain and stress conditions becomes important when the limit of metastability is of concern: under imposed stress, as we will show, a mechanical instability (whose origin is nonetheless thermodynamic) sets in before the spinodal limit identified by Amundson and Helfand for imposed *strain*. Thus, the latter limit is in principle not reachable in a stress experiment. The difference becomes especially pronounced for a (hypothetical) second-order transition. Apart from the emphasis on stress rather than strain, we calculate the full, nonlinear stress–strain curves for both the WSL and SSL. In particular, we study in some detail the undulation of layers under tension, and its consequence on the stress–strain relation, using a nonlinear continuum elastic free energy description derived in this paper for both the weak and strong segregation limits. We show that layer undulation leads to a significant reduction in the (tensile) modulus in both cases. Because of this reduction, melting of the lamellar structure in the WSL occurs at larger strains under tension than under compression.

The paper is organized as follows: We first consider the SSL, as the response of the lamellae is simpler in this limit than in the WSL. In Sec. II, we derive the continuum elastic free energy description of a deformed lamellar structure, based on the deformation free energy of the monolayers comprising the lamellar bulk. We separate the deformation strain into a uniform part and a nonuniform part. Full nonlinearity is retained for the uniform strain, whereas a second-order expansion is performed for the nonuniform part. We then calculate the response of the system to compression and tension, including the undulation patterns formed under tension, and the stress–strain relation. In Sec. III, we study the WSL. Starting with the Brazovskii–Leibler–Fredrickson–Helfand theory for diblock copolymers in the WSL, we derive the free energy in the deformed states, using the phase ansatz and a coarse-grain approximation (to be described in Sec. III A). We then investigate the behavior of the lamellar structure under compression and tension and identify the various types of instabilities. The stress–strain relation for both cases are also calculated and a phase diagram is constructed in terms of a scaled strain and a variable which is related to the temperature or Flory–Huggins parameter. In Sec. IV, we summarize and discuss the main results of the paper.

II. THE STRONG SEGREGATION LIMIT (SSL)

The SSL is obtained when the two blocks, A and B, are sufficiently incompatible, and/or when the blocks are sufficiently long. More quantitatively, this happens when $\chi N \gg 10$ where χ is the Flory–Huggins interaction parameter (in units of k_BT), and N is the degree of polymerization of the diblock. In the SSL, the A and B domains are separated by sharp interfaces, with the junction points of the A–B diblock localized in the narrow interfacial regions. Helfand and Wasserman[12] developed the first systematic

(mean-field) theory for studying this regime. By balancing the interfacial free energy with the elastic free energy of the chains, which was calculated numerically, these authors found that the interdomain spacing D scales as $D\sim N^{2/3}$. This prediction has been found to be in quantitative agreement with electron microscopy and small-angle neutron scattering data.[13] Semenov,[14] exploiting the fact that sufficiently long polymers in the strong segregation limit are strongly stretched beyond their natural radius of gyration, developed an analytical approach for calculating the elastic contribution to the free energy. A very different approach was taken by Ohta and Kawasaki;[15] these authors generalized the order-parameter free energy functional theory of Leibler[16] initially developed for the WSL, by taking account of the long-range interaction which arises from the chain connectivity. Melenkevitz and Muthukumar[17] also studied the strong segregation limit by using a density functional theory based on the Leibler and Ohta and Kawasaki approaches. The order-parameter approaches have been evaluated by Kawasaki and Kawakatsu[18] who raised doubts about the convergence of the order-parameter expansion for the SSL. One advantage of the Ohta and Kawasaki approach, however, is that it enables a systematic derivation of the free energy in the deformed state.[19]

In view of the problematic nature of the order-parameter approach for studying the SSL, we choose to use the Helfand–Wasserman–Semenov approach. These authors however, did not consider the free energy of the deformed lamellar structure. A general deformation of the lamellar structure involves changes in the interlayer spacing as well as curving of the layers. An exact treatment in the framework of Helfand–Wasserman–Semenov remains evasive. However, we note two important, related developments. First, Milner and Witten,[20] and Wang and Safran,[21] have calculated the curvature deformation free energy for a melt polymer monolayer. Wang and Safran have particularly treated the curvature elastic free energy for monolayers of diblock copolymers, taking into account both the interfacial and stretching contributions. Their theory has recently been modified to study certain types of defects in lamellar phases by Gido and Thomas.[22] Second, Turner and Joanny[23] have studied the undulation of a bulk lamellar phase in contact with a rough surface (with a sinusoidally varying profile), using the electrostatic analogy for stretched polymers and an approximation which assumes that the free ends of the copolymers are distributed exclusively at the outer extremities of the monolayers.

In this paper, we follow the approach adopted by Wang and Safran in their study of monolayers and generalize it to the case of bulk lamellae. The key assumptions in the derivation of the deformation free energy of the bulk lamellae are (1) interpenetration of chain segments from two neighboring monolayers is negligible when monolayers are stacked to form the bulk lamellae, and (2) deformations due to (inhomogenous) changes in the layer spacing and due to curvatures are independent and therefore can be treated separately. For a monolayer, the second assumption becomes exactly true at the quadratic order of deformations if curvature is defined at the proper location within the monolayer. Since this is the order that we consider in this paper, we do not expect this assumption to lead to any significant errors. The question of interpenetration has been addressed by Witten *et al.*[6] who showed that the interpenetration zone decreases in a power-law fashion with the degree of polymerization, and becomes vanishingly small in the long chain limit. Although the Turner and Joanny approach is more systematic, for the purpose of this study, it is not necessarily more accurate than ours since it makes no fewer assumptions and approximations. It should be emphasized at this point that, as far as scaling is concerned, any of the above mentioned approaches, including the Ohta and Kawasaki approach, will give the same results; the differences are only in the numerical prefactors.

A. Free energy of the deformed lamellae

We start from considering the free energy of a single symmetric diblock copolymer monolayer. We assume $N_A=N_B=(1/2)N$, $v_A=v_B=v$, and $a_A=a_B=a$, where v is the monomeric volume and a is the Kuhn length. The free energy per chain of a flat monolayer is[21]

$$\tilde{f}=\gamma\Sigma+\frac{\pi^2}{24}\frac{Nv^2k_BT}{a^2\Sigma^2}, \tag{2.1}$$

where γ is the interfacial tension between the A and B blocks,[24] and Σ is the area per chain at the surface of the junction points.

First, we change the above free energy per chain to a free energy per unit volume. This is accomplished by noting that the volume of a copolymer chain is Nv, so we can simply divide Eq. (2.1) by Nv. Next, we eliminate Σ in favor of the thickness of the monolayer D by using the (bulk) incompressibility condition $\Sigma D=Nv$. Thus we arrive at the following free energy per unit volume:

$$f=\frac{\gamma}{D}+\frac{\pi^2}{24}\frac{D^2k_BT}{N^2a^2v} \tag{2.2}$$

for any layer thickness D. The total free energy of a stack of monolayers under uniform dilation or compression can be obtained by integrating the free energy density Eq. (2.2) over the volume of the system. Note that in the multilayer system, D can also be thought of as the distance from one A–B junction surface to the next A–B junction surface. Thus a change in D can be identified as a change in the interlayer spacing. (Note here we are using the distance between two adjacent *monolayers* since we are considering completely symmetric diblocks; in general we should use *bilayers* as the units of the the lamellae.)

If the interlayer distance is changed from D to $D+\Delta D$, the free energy density becomes

$$f(D+\Delta D)=f(D)+\left(-\frac{\gamma}{D}+\frac{\pi^2}{12}\frac{D^2k_BT}{N^2a^2v}\right)e+\frac{1}{2}\left(\frac{2\gamma}{D}+\frac{\pi^2}{12}\frac{D^2k_BT}{N^2a^2v}\right)e^2+O(e^3), \tag{2.3}$$

where $e=\Delta D/D$. Note that in the above considerations, D is not necessarily the equilibrium spacing, thus Eq. (2.3) can be regarded as an expansion of the free energy around any uniformly strained state, of which the equilibrium one is a special case, and likewise, the strain e is defined on top of the uniformly strained state, i.e., with respect to a general interlayer spacing D. The reason for expanding the free energy this way is that we want to eventually separate the total strain into a uniform part and a nonuniform part e, and to be able to treat situations where the uniform part can be large even though the nonuniform part is small.

The equilibrium spacing D_0 is obtained by locating the minimum of Eq. (2.1) or Eq. (2.2) which yields,

$$D_0=(12/\pi^2)^{1/3}(\gamma/k_BT)^{1/3}N^{2/3}a^{2/3}v^{1/3} \tag{2.4}$$

with the minimum of the free energy (per unit volume) equal to

$$\begin{aligned} f_0&=f(D_0)\\ &=\tfrac{3}{2}(\pi^2/12)^{1/3}(\gamma/k_BT)^{2/3}N^{-2/3}a^{-2/3}v^{-1/3}k_BT. \end{aligned} \tag{2.5}$$

If we now define $r=D/D_0$, the free energy of the deformed state becomes

$$\begin{aligned} f(D+\Delta D)=&\frac{2}{3}f_0\left(\frac{1}{r}+\frac{r^2}{2}\right)+\frac{2}{3}f_0\left(-\frac{1}{r}+r^2\right)e\\ &+\frac{2}{3}f_0\left(\frac{1}{r}+\frac{r^2}{2}\right)e^2. \end{aligned} \tag{2.6}$$

Let us now consider the curvature deformation. The free energy per chain for a curvature c is[20,21]

$$\tilde{f}_c=\frac{\pi^2}{128}\frac{N^3v^4k_BT}{a^2\Sigma^4}c^2=\frac{\pi^2}{128}\frac{D^4k_BT}{Na^2}c^2. \tag{2.7}$$

The free energy per unit volume f_c is again obtained by dividing Eq. (2.7) by the volume of the copolymer Nv. If we make use of Eqs. (2.4) and (2.5), we get

$$f_c=\tfrac{1}{16}f_0\ r^4D_0^2c^2. \tag{2.8}$$

For a symmetric monolayer, the surface of the junction points of the two blocks is a neutral surface.[25] Thus if we define the curvature c on this surface, the deformations due to the change in spacing e and due to the curvature c are decoupled; the total deformation free energy is simply the sum of the two contributions. The elastic constants can be extracted from the coefficients of the quadratic terms e^2 and c^2, and we find

$$B=\frac{4}{3}f_0\left(\frac{1}{r}+\frac{r^2}{2}\right) \tag{2.9a}$$

for the compression modulus and

$$K=\tfrac{1}{8}f_0r^4D_0^2 \tag{2.9b}$$

for the bending modulus.

We now introduce the displacement $u(z;\mathbf{r}_\perp)$ as $u(z;\mathbf{r}_\perp)=h(z;\mathbf{r}_\perp)-z$, where $h(z;\mathbf{r}_\perp)=h(nD;\mathbf{r}_\perp)$ is the height of the nth layer, and $\mathbf{r}_\perp$ is the coordinate in the transverse directions. The Lagrange strain due to the displacement u is

$$\begin{aligned} e&=(\partial_z h)[1+(\nabla_\perp h)^2]^{-1/2}-1\\ &=[1+(\nabla_\perp u)^2]^{-1/2}+(\partial_z u)[1+(\nabla_\perp u)^2]^{-1/2}-1\\ &\approx\partial_z u-\tfrac{1}{2}(\nabla_\perp u)^2. \end{aligned} \tag{2.10}$$

The curvature corresponding to u is

$$\begin{aligned} c&=\nabla_\perp\cdot\{(\nabla_\perp h)[1+(\nabla_\perp h)^2]^{-1/2}\}\\ &=\nabla_\perp\cdot\{(\nabla_\perp u)[1+(\nabla_\perp u)^2]^{-1/2}\}\\ &\approx\nabla_\perp^2 u. \end{aligned} \tag{2.11}$$

Thus, we have finally the nonlinear free energy for a general deformation $u(z;\mathbf{r}_\perp)$,

$$\begin{aligned} F=&\frac{2}{3}f_0\left(\frac{1}{r}+\frac{r^2}{2}\right)V+\int d\mathbf{r}\Big\{B'\left[\partial_z u-\frac{1}{2}(\nabla_\perp u)^2\right]\\ &+\frac{1}{2}B\left[\partial_z u-\frac{1}{2}(\nabla_\perp u)^2\right]^2+\frac{1}{2}K(\nabla_\perp^2 u)^2\Big\}, \end{aligned} \tag{2.12}$$

where V is the volume of the sample, $B'=(2/3)f_0(-r^{-1}+r^2)$, and B and K are given by Eqs. (2.9a) and (2.9b), respectively.

In this paper, we will only consider situations where uniform strains, as well as nonuniform strains, are both small. In these cases, it suffices to expand the free energy up to the second order in the uniform strain $\epsilon=r-1$, defined with respect to the undeformed, equilibrium state. At this order, the free energy of the deformed lamellae becomes

$$\begin{aligned} F=&\int d\mathbf{r}\Big\{f_0+f_0\left[\epsilon+\partial_z u-\frac{1}{2}(\nabla_\perp u)^2\right]^2\\ &+\frac{1}{16}f_0D_0^2(\nabla_\perp^2 u)^2\Big\}. \end{aligned} \tag{2.13}$$

Thus the compression and bending moduli at the equilibrium state, are respectively,

$$B_0=2f_0=3(\pi^2/12)^{1/3}(\gamma/k_BT)^{2/3}N^{-2/3}a^{-2/3}v^{-1/3}k_BT \tag{2.14a}$$

and

$$K_0=\tfrac{1}{8}f_0D_0^2=\tfrac{3}{16}(12/\pi^2)^{1/3}(\gamma/k_BT)^{4/3}N^{2/3}a^{2/3}v^{1/3}k_BT. \tag{2.14b}$$

If we take $\gamma=0.006k_BT/\text{Å}^2$, $a=7.5$ Å, $v=113$ Å^3, $N=1000$,[26] and $T=350$ K, we obtain $D_0\approx36$ nm, $f_0\approx1.2\times10^6$ dyn/cm^2, and therefore, $B_0\approx2.4\times10^6$ dyn/cm^2 and $K_0\approx2.0\times10^{-6}$ dyn. As in the study of smetics, one may define a length scale $\Lambda=(K_0/B_0)^{1/2}$. From Eqs. (2.14a) and (2.14b), we see that $\Lambda=(1/4)D_0$. Since D_0 is the thickness of the monolayer, which is half the period of the lamellar structure, Λ is 12.5% of the periodicity of the lamellae.

Note that even though the free energy Eq. (2.13) is the result of an expansion of the strain to the second order, it is nonlinear in the displacement $u(z;\mathbf{r}_\perp)$ through the nonlinear dependence of the strain on u, Eq. (2.10). The choice of keeping only the leading nonlinearity arising from Eq. (2.10) while ignoring the others is partially justified by an analysis of the length scales over which u varies in the layer normal and transverse directions; the form of Eq. (2.13) is further corroborated by the form of the free energy of the deformed lamellar phase in the WSL which is derived using a very different method in Sec. III A.

We now use Eq. (2.13) to analyze separately the response of the system to uniaxial compression and tension.

B. Compression

Let L_0 denote the dimension of the system in the layer normal direction (which we take to be the z-direction) in the undeformed state, and let L denote the same dimension in the deformed state. To enable a unified treatment of compression and tension, we define the strain as $\epsilon = L/L_0 - 1$, so that a positive strain corresponds to tension and a negative strain corresponds to compression. Correspondingly, we define the stress to be positive for tension and negative for compression.

In the case of compression, we do not expect any undulation in u (for small strains). The free energy density, from Eq. (2.13) is simply

$$f = f_0 + f_0\epsilon^2. \tag{2.15}$$

The stress σ is simply the derivative of the free energy with respect to the strain

$$\sigma = \frac{df}{d\epsilon} = 2 f_0\epsilon = B_0\epsilon \tag{2.16}$$

as one would expect when the curvature $c=0$. Alternatively, the stress–strain relation Eq. (2.16) can be obtained from the Gibbs free energy density,[27]

$$g = f - \eta L/V, \tag{2.17}$$

where η is the *force* applied to the system in the z-direction. Because the fluid as a whole is incompressible, $V = L_0 S_0$, where S_0 is the cross-sectional area of the undeformed sample. Using our definition of the strain, and defining the stress as $\sigma = \eta/S_0$, we can write the Gibbs free energy density as

$$g = f(\epsilon) - \sigma(1+\epsilon). \tag{2.18}$$

For a given stress, the strain is obtained from minimizing the above Gibbs free energy. The result is, of course, identical to Eq. (2.16).

C. Tension

Buckling of smectics under tension in the layer normal direction has been studied both theoretically and experimentally.[7–10] Though not emphasized in the literature, this phenomenon is due, in large part, to the boundary effects. In a truely translationally invariant system, the system can simply make a uniform tilt of the layers, or make a single cusp,[28] with no or little energy cost. When the system is confined to two parallel walls which are also parallel to the layers, the layers on the top and bottom are forced to conform with the flatness of the two boundaries, thereby excluding the possibility of uniform tilt, or a cusp of macroscopic size. In other words, inhomogeneity in the z direction, for example, the condition that $u=0$ at the two boundaries, is crucial. We first carry out a linear stability analysis using Eq. (2.13), keeping terms only up to the quadratic order in the spatial derivatives of the displacement. Following Delrieu[8] and de Gennes,[7] we make the simple ansatz that the displacement u in the buckled state can be described by

$$u = u_0 \sin(\kappa z)\cos(kx), \tag{2.19}$$

where $\kappa = \pi/L$ ensuring that u vanishes on both boundaries at $z=0$ and $z=L$. The ansatz is reasonable if the strain is not too large and if L is less than a correlation length ξ, the length scale over which a surface undulation propogates into the bulk.[7] For a sinusoidal surface undulation of wave number k, $\xi \sim 1/(k^2\Lambda)$, where $\Lambda = (K/B)^{1/2}$. It turns out that in the situations we study, the latter condition will always be only marginally satisfied. More elaborate trial functions can of course be constructed; however they are not expected to significantly change the conclusions derived from using Eq. (2.19). Therefore, in the interest of simplicity and transparency of analysis, we will adhere to the ansatz Eq. (2.19).

We consider the free energy per unit volume. For an inhomogeneous system this is obtained by integrating over the sample and then dividing by the volume. To quadratic orders in the displacement, we have

$$f = \tfrac{1}{2}B_0\epsilon^2 + B_0\epsilon[\langle\partial_z u\rangle - \tfrac{1}{2}\langle(\partial_x u)^2\rangle] + \tfrac{1}{2}B_0\langle(\partial_z u)^2\rangle + \tfrac{1}{2}K_0\langle(\partial_x^2 u)^2\rangle, \tag{2.20}$$

where $\langle\cdots\rangle$ denotes the aforementioned spatial average. In Eq. (2.20), we have ignored the unimportant constant term f_0. The term $\langle\partial_z u\rangle$ vanishes by the boundary condition; other terms can be evaluated in a straightforward way. We obtain

$$f = \tfrac{1}{2}B_0\epsilon^2 + \tfrac{1}{8}(-B_0\epsilon k^2 + B_0\kappa^2 + K_0 k^4)u_0^2 \equiv \tfrac{1}{2}B_0\epsilon^2 + Q(\epsilon,k)u_0^2. \tag{2.21}$$

The undulation instability sets in when the minimum of $Q(\epsilon,k)$ first becomes negative for a certain wave vector k at some critical strain ϵ_c. From $\partial Q(\epsilon,k)/\partial k = 0$ and $Q(\epsilon,k) = 0$, we find

$$\epsilon_c = 2\kappa\sqrt{K_0/B_0} = 2\kappa\Lambda = 2\pi\Lambda/L, \tag{2.22a}$$

and

$$k = \sqrt{\kappa/\Lambda} = \sqrt{\pi/\Lambda L} \tag{2.22b}$$

in agreement with the results for smectics.[7]

To find the amplitude of the undulation, we need to keep the nonlinear terms in u. Using Eq. (2.13) and after some straightforward algebra, we find

$$u_0=\frac{8}{3}\sqrt{\frac{\Lambda L}{2\pi}}(\epsilon-\epsilon_c)^{1/2}. \tag{2.23}$$

The wave vector of the undulation can be shown to be unaltered by the nonlinear terms. The strain free energy now becomes

$$f=\tfrac{1}{2}B_0\epsilon^2-\tfrac{2}{9}B_0(\epsilon-\epsilon_c)^2. \tag{2.24}$$

Note that the length scale for u_0 is the same as the wavelength of undulation.

Using a continuum free energy similar to Eq. (2.13), Delrieu[8] showed that the square-lattice wave is the lowest free energy state. For the square-lattice wave, we make the following ansatz:

$$u=\frac{1}{\sqrt{2}}u_0\sin(\kappa z)[\cos(kx)+\cos(ky)]. \tag{2.25}$$

The critical strain and the wave vector of undulation are again given by Eqs. (2.22a) and (2.22b), respectively. Beyond the critical strain, however, the amplitude of the undulation is given by

$$u_0=8\sqrt{\frac{\Lambda L}{15\pi}}(\epsilon-\epsilon_c)^{1/2} \tag{2.26}$$

and the total strain free energy beyond the critical strain ϵ_c is

$$f=\tfrac{1}{2}B_0\epsilon^2-\tfrac{4}{15}B_0(\epsilon-\epsilon_c)^2. \tag{2.27}$$

Because the strain free energy for the square-lattice wave is lower than that for the one-dimensional wave, we use Eq. (2.27) as the free energy for the post-critical-strain state. Below the critical strain, there is no undulation in u, so the strain free energy is simply the first term of Eq. (2.27). Because stress is the derivative of the free free energy with respect to strain, in passing through the critical strain, the stress–strain curve undergoes a discontinuity in its slope, i.e., a sudden change in the modulus. Below the critical strain, the stress–strain relation is

$$\sigma=B_0\epsilon \tag{2.28a}$$

with a modulus B_0, whereas above the critical strain, it is given by

$$\sigma=B_0\epsilon-\tfrac{8}{15}B_0(\epsilon-\epsilon_c)=\tfrac{7}{15}B_0\epsilon+\tfrac{8}{15}B_0\epsilon_c \tag{2.28b}$$

with a modulus 7/15 of the precritical state. Since the above analysis did not assume any particular form for B_0 and K_0, this result should be quite general. The only dependence on the particular system is the value of the critical strain ϵ_c.

The full stress–strain curve is shown in Figs. 2(a) and 2(b), in which we have also included the portion corresponding to compression. Because the critical strain is usually very small for typical experimental situations—for example, if we take the sample thickness L to be 2 mm ($\kappa=\pi/L=0.5\pi\ \mathrm{mm}^{-1}$), with layer spacing $D_0=36$ nm ($\Lambda=9$ nm), then $\epsilon_c=2.83\times10^{-5}$—the apparent tensile stress–strain curve in an experimental measurement should correspond to the postcritical regime. In other words, the modulus for tension and compression will appear different, the former being 7/15 of the later.

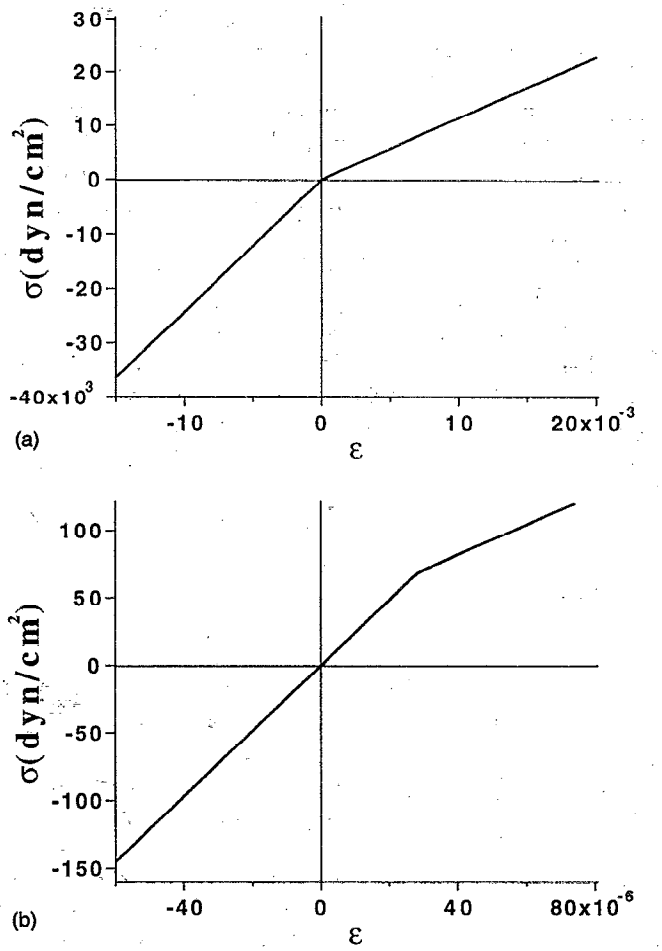

FIG. 2. A representative stress–strain curve for a model diblock copolymer lamellar structure in the strong segregation limit. Parameters used are $N=1000$, $a=7.5$ Å, $v=113$ Å^3, $\gamma=0.006\ k_BT$, and $T=350$ K. (b) is a close-up view of the small strain region, showing the buckling instability at some critical strain. The thickness of the sample is taken as $L=2$ mm.

III. THE WEAK SEGREGATION LIMIT (WSL)

Microphase separation of diblock copolymers in the weak segregation limit was first studied by Leibler.[16] For a symmetric A–B diblock copolymer of N segments (we assume that the two blocks have the same geometric characteristics, namely, the same segmental length a and monomeric volume v), with a Flory–Huggins interaction parameter χ (scaled by k_BT), the effective Hamiltonian for the composition variation is given by[16]

$$\frac{H[\phi(\mathbf{r})]}{k_BT}=\int d\mathbf{r}\left\{\frac{1}{2}\tau\psi^2+\frac{1}{2}s[(q_0^4\psi^2-2q_0^2(\nabla\psi)^2+(\nabla^2\psi)^2]+\frac{\mu}{4!}\psi^4\right\}. \tag{3.1}$$

In the equation above, $\psi=\alpha\bar{N}^{-1/4}\phi$ is the scaled order-parameter, with $\phi(\mathbf{r})=\phi_A(\mathbf{r})-1/2$ measuring the local deviation of the volume fraction of one type of monomers,

say A, from the bulk composition 1/2, $\tau=2[(\chi N)_s-\chi N]/\alpha^2$, where $(\chi N)_s$ is the value of the combination χN at the mean-field spinodal, $\mu=\lambda\bar{N}^{-1/2}$ with $\bar{N}=Na^6/v^2$, q_0 is the scaled wave number at the peak position of the structure factor computed by Leibler, and the position $\mathbf{r}$ has been scaled by the end-to-end distance $N^{1/2}a$. $\alpha=1.1019$ and $\lambda=106.18$ are numerical parameters evaluated at the symmetric composition. For symmetric diblocks, $s=1/(24b^*)$, $q_0^2=6b^*$, with $b^*=3.7852$, and $(\chi N)_s=10.495$.

Leibler used a Landau approximation (the tree approximation), replacing $\psi(\mathbf{r})$ with $\bar{\psi}(\mathbf{r})\equiv\langle\psi(\mathbf{r})\rangle$ in the Hamiltonian $H(\psi)$ and equating $H(\bar{\psi})$ with the Helmholtz free energy $F(\bar{\psi})$. In the vicinity of the order–disorder transition, the order-parameter is assumed to be described by

$$\bar{\phi}(\mathbf{r})=2A\cos(qz) \tag{3.2}$$

and the (dimensionless) free energy density $f(A,q)$ becomes

$$f(A,q)=[\tau+s(q^2-q_0^2)^2]A^2+(1/4)\mu A^4. \tag{3.3}$$

For $\tau<0$, the equilibrium amplitude A is given by $A^2=2|\tau|/\mu$, with the wave number $q=q_0$.

The Hamiltonian Eq. (3.1) belongs to the class of Brazovskii models.[29] As pointed out by Brazovskii and Leibler, thermal fluctuations around the optimal wave number q_0 become very large near the mean-field spinodal; these fluctuations renormalize the transition between isotropic and lamellar phases from a second-order one to a weakly first-order one. Fredrickson and Helfand[30] treated the effects of fluctuations explicitly by a one-loop Hartree approximation, and showed that the transition from the isotropic phase to the lamellar phase indeed becomes weakly first-order, the discontinuity in the order parameter at the transition decreasing with increasing degree of polymerization. A series version of the fluctuation-renormalized free energy functional has been proposed by Fredrickson and Binder.[31] To the sixth power in the order-parameter, the free energy reads

$$\frac{F[\phi(\mathbf{r})]}{k_BT}=\int d\mathbf{r}\left\{\frac{1}{2}\tau_R\bar{\psi}^2+\frac{1}{2}s[(q_0^4\bar{\psi}^2)-2q_0^2(\nabla\bar{\psi})^2+(\nabla^2\bar{\psi})^2]+\frac{\mu_R}{4!}\bar{\psi}^4+\frac{\omega_R}{6!}\bar{\psi}^6\right\}, \tag{3.4}$$

where the renormalized parameters τ_R, μ_R, and ω_R are given by

$$\tau_R=\tau+d\mu\tau_R^{-1/2}, \tag{3.5a}$$

$$\mu_R=\mu(1-\tfrac{1}{2}d\mu\tau_R^{-3/2})(1+\tfrac{1}{2}d\mu\tau_R^{-3/2})^{-1}, \tag{3.5b}$$

$$\omega_R=\tfrac{9}{2}d\mu^3\tau_R^{-5/2}(1+\tfrac{1}{2}d\mu\tau_R^{-3/2})^{-3}, \tag{3.5c}$$

with $d=3b^*/2\pi$.

An important feature of the free energy Eq. (3.4) is that near the (renormalized) order–disorder transition, the paramter μ_R is negative. Thus, when substituting the ansatz for the order parameter Eq. (3.2) into Eq. (3.4), the (dimensionless) free energy density

$$f(A,q)=[\tau_R+s(q^2-q_0^2)^2]A^2+(1/4)\mu_RA^4+(1/36)\omega_RA^6 \tag{3.6}$$

has the feature of a triple-well potential. The transition from the isotropic phase ($A=0$) to the lamellar phase takes place when $\mu_R^2-(16/9)\tau_R\omega_R=0$, and the spinodal where the lamellar phase loses its metastability is at $\mu_R^2-(4/3)\tau_R\omega_R=0$. The square of the amplitude of the composition wave is given [for $\mu_R^2>(4/3)\tau_R\omega_R$] by

$$A^2=3[(\mu_R^2-\tfrac{4}{3}\tau_R\omega_R)^{1/2}-\mu_R]/\omega_R \tag{3.7}$$

and the optimal wave vector is again at $q=q_0$.[32] In our paper, we will use the series version of the renormalized free energy Eq. (3.4). However, we will also study the consequences of the Landau free energy Eq. (3.3) where the mechanical instability is most dramatic.

Near the transition region, $d\mu\tau_R^{-3/2}\equiv d\lambda\bar{N}^{-1/2}\tau_R^{-3/2}$ is $O(1)$. Therefore, although experimentally the controlling variables are N and χN, theoretically, it is more natural and convenient to define $m=d\lambda\bar{N}^{1/2}\tau_R^{-3/2}$, and use this combination and N as the controlling parameters. This will enable us to see more clearly the scaling of various properties as a function of N. In terms of m and N, Eqs. (3.5a), (3.5b), and (3.5c) become

$$\tau_R=m^{-2/3}(d\lambda)^{2/3}\bar{N}^{-1/3}(1-m), \tag{3.8a}$$

$$\mu_R=\lambda\bar{N}^{-1/2}(1-m/2)(1+m/2)^{-1}, \tag{3.8b}$$

$$\omega_R=(9/2)(\lambda^2/d)^{2/3}\bar{N}^{-2/3}m^{5/3}(1+m/2)^{-3}. \tag{3.8c}$$

The thermodynamic transition point is located at $m_t=9.2544$ and the spinodal for the lamellar phase is at $m_s=8.2129$, independent of N. In terms of m and N, Eq. (3.7) becomes

$$A^2=\tfrac{2}{3}(d^2/\lambda)^{1/3}av^{-1/3}N^{1/6}\tilde{h}(m), \tag{3.9}$$

where

$$\tilde{h}(m)=m^{-5/3}\{[(1-m/2)^2(1+m/2)^4-6m(1+m/2)^3]^{1/2}-(1-m/2)(1+m/2)^2\}. \tag{3.10}$$

It should already become clear from Eqs. (3.6) and (3.7), that if the wave vector q is constrained to be different from q_0, then the amplitude of the order-parameter will decrease and the free energy of the constrained lamellar phase increase. This is precisely the situation which obtains when the lamellae are subjected to a mechanical strain or stress directed along the layer normal. For compression, we can simply relate q to the imposed strain ($q=q_0$ corresponds to the strain-free state) and use Eqs. (3.6) and (3.7) to study the quasistatic behavior of the lamellar phase. In this case, the response is expected to be a decrease in the amplitude of the composition wave and eventually the "melting" of the lamellar phase under sufficiently large strains. For tensile strains, however, the situation is more subtle, as the layers can first buckle before they melt. Thus, we need to study, in addition to changes in the amplitude, also changes in the phase of the wave.

This requires that we derive an expression of the free energy for treating more general deformations.

A. Free energy of the deformed lamellae

To derive the free energy of the deformed states, we make the phase approximation, i.e., we assume that the lamellae are described by a composition wave with a position-dependent phase but a position-independent amplitude

$$\bar{\psi}(\mathbf{r})=2A\cos\{q[z+u(z;\mathbf{r}_\perp)]\}. \tag{3.11}$$

For small displacement (phase shift) $u(z;\mathbf{r}_\perp)$, we can make a coarse-grain approximation which amounts to averaging a slowly-varying function over one or several layers. This procedure is illustrated in the following.

Take, for example, the term $[\nabla\bar{\psi}(\mathbf{r})]^2$. A straightforward calculation using Eq. (3.11) yields

$$[\nabla\bar{\psi}(\mathbf{r})]^2=4A^2q^2[(1+\partial_z u)^2+(\nabla_\perp u)^2]\times\sin^2[qz+qu(z;\mathbf{r}_\perp)]. \tag{3.12}$$

Using trigonometric relations, we can write

$$\sin^2[qz+qu(z;\mathbf{r}_\perp)]=\tfrac{1}{2}-\tfrac{1}{2}\{\cos(2qz)\cos[2qu(z;\mathbf{r}_\perp)]-\sin(2qz)\sin[2qu(z;\mathbf{r}_\perp)]\}. \tag{3.13}$$

We now average Eq. (3.12) over a full period in z. Because u is small, the function $\cos[2qu(z;\mathbf{r}_\perp)]$ varies slowly. The coarse-grain approximation then treats any slowly-varying function $\theta(z;\mathbf{r}_\perp)$ as constant when averaging over a period. Thus,

$$\frac{\int_z^{z+2\pi/q}dz'\,\theta(z';\mathbf{r}_\perp)\cos(mqz')}{\int_z^{z+2\pi/q}dz'}\approx\theta(z;\mathbf{r}_\perp)\frac{\int_z^{z+2\pi/q}dz'\cos(mqz')}{\int_z^{z+2\pi/q}dz'}=\theta(z;\mathbf{r}_\perp)\delta_{m,0} \tag{3.14}$$

for any integer m. In the frame work of this approximation, only terms in the free energy which involve spatial derivatives of the order-parameter give rise to $u(z;\mathbf{r}_\perp)$-dependent contributions; local terms remain independent of u. After some straightforward algebra as outlined above, we obtain the free energy for deformed lamellae as

$$f[A,q,u(\mathbf{r})]=f_0(A)+(1/V)A^2s\int d\mathbf{r}\{[q^2(1+\partial_z u)^2+q^2(\nabla_\perp u)^2-q_0^2]^2+q^2(\partial_z^2u+\nabla_\perp^2 u)^2\}, \tag{3.15}$$

where $f_0(A)$ is the local part of the free energy density Eq. (3.6).

We now simplify Eq. (3.15) to an expression valid for small strains. The layer spacing corresponding to the unconstrained equilibrium lamellae is $D_0=2\pi/q_0$. If the dimension of the sample in the z-direction (the layer normal direction) is L_0, then the number of layers in the system is $L_0/D_0=(q_0L)/(2\pi)$. Since we are considering a quasistatic equilibrium with fixed number of layers, we have $L_0/D_0=L/D$ with the new spacing given by $D=2\pi/q$. Thus, $L/L_0\equiv 1+\epsilon=q_0/q$, and for small ϵ, $q_0^2-q^2\approx 2q_0^2\epsilon$. From our analysis in the previous section, we see that $\nabla_\perp u\sim ku_0=u_0\sqrt{\pi/(\Lambda L)}$, while $\partial_z u\sim u_0/L$ [cf. Eq. (2.19)]. Thus we can neglect the term $(\partial_z u)^2$ in comparison with the term $(\nabla_\perp u)^2$ in the square bracket in Eq. (3.15), and the term $\partial_z^2 u$ in comparison with the term $\nabla_\perp^2 u$. Furthermore, since $u_0\sim\epsilon^{1/2}$ if there is layer undulation [cf. Eq. (2.26)], we can replace any q factor that multiplies the spatial derivatives of u by q_0; the corrections will be higher than quadratic in ϵ. These claims can all be verified by a more detailed analysis of Eq. (3.14), which we choose to omit in the presentation. Under the provision of these approximations, Eq. (3.15) becomes

$$f[A,\epsilon,u(\mathbf{r})]=f_0(A)+(1/V)A^2s\int d\mathbf{r}\{4q_0^4[\epsilon+\partial_z u-(\nabla_\perp u)^2]^2+q_0^2(\nabla_\perp^2 u)^2\}, \tag{3.16}$$

where we have changed u to $-u$. Notice that the strain-dependent term has the same form as Eq. (2.13), with the identification of the moduli $B_B=8sq_0^4A^2$ and $K_B=2sq_0^2A^2$ or in dimensional units

$$B_B=8sq_0^4A^2k_BT/(N^{3/2}a^3) \tag{3.17a}$$

and

$$K_B=2sq_0^2A^2Na^2k_BT/(N^{3/2}a^3), \tag{3.17b}$$

where the subscript B indicates that these are "bare" moduli in the sense that A depends on the strain. For very small strains, the dependence of A on ϵ enters in higher-order corrections; therefore B_B and K_B can be regarded as the initial moduli for infinitesimal deformations. Using Eqs. (3.9) and (3.10), and the numerical values for s, q_0^2, d, and λ, these elastic moduli can be written as

$$B_B=9.488\,2a^{-2}v^{-1/3}N^{-4/3}\tilde{h}(m)k_BT \tag{3.18a}$$

and

$$K_B=0.104\,44v^{-1/3}N^{-1/3}\tilde{h}(m)k_BT. \tag{3.18b}$$

If we use $a=7.5$ Å, $v=113$ Å^3, and $N=1000$, and $T=350$ K (as in Sec. II A), we estimate these elastic constants to be 7.1×10^5 dyn/cm^2 and 4.4×10^{-8} dyn, respectively, at the thermodynamic transition point ($m=9.2544$). The length scale Λ arising from the combination $\sqrt{K_B/B_B}$ is $\Lambda=1/(2q_0)=D_0/4\pi$ which agrees with Amundson and Helfand.[11]

We note from Eqs. (3.18a) and (3.18b), that both elastic moduli vanish in the long chain limit for finite m; this is another manifestation that in the limit of infinitely long chains, the weakly first-order transition approaches a second-order one. Interestingly, though, the vanishing of these elastic constants near the order–disorder transition does not imply that the ordered phase becomes less stable. In fact, Morse and Milner[33] have argued that the opposite is true because the dislocation line energy per persistence length in the ordered phase diverges as $N^{1/6}$ in the long chain limit.

We now use our free energy Eq. (3.16) to discuss the behavior of the lamellar phase under compression and tension, respectively.

B. Compression

Under uniaxial compression in the direction of the layer normal, only the layer spacing and the amplitude of the composition wave are expected to change; there is no layer undulation, so $u_z=u_x=u_y=0$ and $u_{zz}=u_{xx}=u_{yy}=0$. Thus, Eq. (3.16) reduces to Eq. (3.6) and the free energy density becomes

$$f(A,\epsilon)=(\tau_R+4sq_0^4\epsilon^2)A^2+(1/4)\mu_R A^4+(1/36)\omega_R A^6. \tag{3.19}$$

The order parameter A^2 for a given strain is now

$$A^2=3\{[\mu_R^2-\tfrac{4}{3}(\tau_R+4sq_0^4\epsilon^2)\omega_R]^{1/2}-\mu_R\}/\omega_R. \tag{3.20}$$

Thus, the effect of a finite strain is to decrease the magnitude of the order parameter, which is equivalent to an upward shift of τ_R (for fixed μ_R and ω_R). This analogy immediately leads us to the following conclusions:

(1) The first order transition where the free energy of the isotropic phase is the same as the free energy of the lamellar phase is now shifted to

$$\mu_R^2=\tfrac{16}{9}(\tau_R+4sq_0^4\epsilon^2)\omega_R, \tag{3.21}$$

so the critical strain for this quasithermodynamic (QT) transition is

$$\epsilon_{QT}=\frac{1}{2s^{1/2}q_0^2}\left(\frac{9\mu_R^2}{16\omega_R}-\tau_R\right)^{1/2}$$

$$=\frac{1}{2s^{1/2}q_0^2}(d\lambda)^{1/3}v^{1/3}a^{-1}N^{-1/6}\tilde{\epsilon}_{QT}(m) \tag{3.22}$$

with

$$\tilde{\epsilon}_{QT}(m)=m^{-5/6}[\tfrac{1}{8}(1-m/2)^2(1+m/2)-m]^{1/2}. \tag{3.23}$$

(2) The spinodal (SP) where the lamellar phase loses its metastability is now shifted to

$$\mu_R^2=\frac{4}{3}(\tau_R+4q_0^4\epsilon^2)\omega_R, \tag{3.24}$$

so the critical strain for this metastability limit is

$$\epsilon_{SP}=\frac{1}{2s^{1/2}q_0^2}\left(\frac{3\mu_R^2}{4\omega_R}-\tau_R\right)^{1/2}$$

$$=\frac{1}{2s^{1/2}q_0^2}(d\lambda)^{1/3}v^{1/3}a^{-1}N^{-1/6}\tilde{\epsilon}_{SP} \tag{3.25}$$

with

$$\tilde{\epsilon}_{SP}(m)=m^{-5/6}[\tfrac{1}{6}(1-m/2)^2(1+m/2)-m]^{1/2}. \tag{3.26}$$

Note that $\epsilon_{SP}>\epsilon_{QT}$. Also note the scaling of these critical strains with the degree of polymerization N for fixed m.

Based on the above discussion, we obtain the following scenario for a lamellar structure under compressional strain in the WSL slightly below the thermodynamic disorder–order transition: As the compressional strain is increased, the amplitude of the composition wave deceases. If the nucleation barrier is not high, then at a critical strain given by Eq. (3.22), the lamellar phase will undergo a quasithermodynamic melting to the isotropic state (with a subsequent reorganization into the equilibrium lamellar structure corresponding to the new dimensions of the sample; see discussions in Sec. IV). If the nucleation barrier is high, or if the rate of strain increase is fast enough to preempt the nucleation of the isotropic phase (and yet still slow enough for maintaining local equilibrium), then the strain can be increased beyond ϵ_{QT}, to ϵ_{SP} at which point the system reaches the spinodal and will melt directly into the isotropic phase (again with a subsequent reorganization into the equilibrium lamellar structure corresponding to the new dimensions of the sample). These conclusions are in agreement with Amundson and Helfand.[11]

When the system is subjected to a given *stress* rather than a given strain, the Helmholtz free energy density Eq. (3.19) is no longer the appropriate thermodynamic potential. The new thermodynamic potential has to reflect the work that is being done on the system by the compressional (or tensile) force. This is accomplished by introducing a Gibbs free energy density

$$g(A,\epsilon;\eta)\equiv f(A;\epsilon)-\eta L/V, \tag{3.27}$$

where η is the *force* along the direction of the layer normal, defined positive for tension and negative for compression. Defining the stress σ as $\sigma=\eta/S_0$, where S_0 is the lateral area of the strain-free state, we again have [cf. Eqs. (2.17) and (2.18)]

$$g(A,\epsilon;\sigma)=f(A;\epsilon)-\sigma(1+\epsilon). \tag{3.28}$$

The equilibrium A and ϵ for a fixed σ are obtained from

$$\partial g/\partial A=0 \tag{3.29a}$$

and

$$\partial g/\partial\epsilon=0. \tag{3.29b}$$

Equation (3.29a) is the same as Eq. (3.20) where the strain ϵ is obtained from Eq. (3.29b) which, when written explicitly, reads

$$\sigma=8sq_0^4A^2\epsilon. \tag{3.30}$$

Equation (3.30) is the stress–strain relation for the lamellar phase. Since A^2 depends on ϵ, the stress–strain relation Eq. (3.29) is intrinsically nonlinear.

In order that the equilibrium state specified by Eqs. (3.29a) and (3.29b) is stable (at least locally), the second derivatives of the free energy must satisfy the following inequality:

$$\left(\frac{\partial^2 g}{\partial A^2}\right)\left(\frac{\partial^2 g}{\partial\epsilon^2}\right)-\left(\frac{\partial^2 g}{\partial A\partial\epsilon}\right)^2>0. \tag{3.31}$$

Equivalently, we can write the stability condition as the slope of the stress–strain relation being always positive,

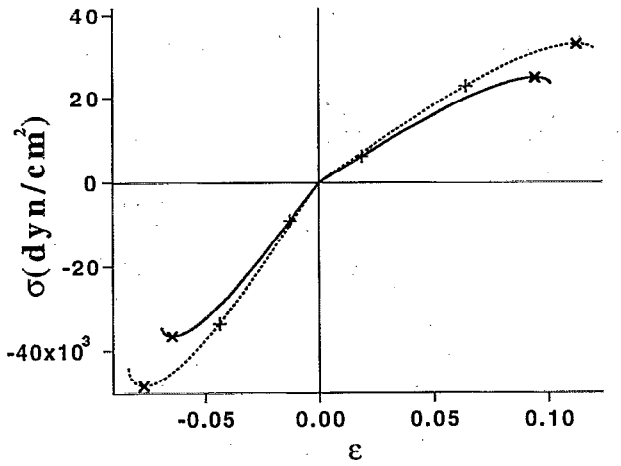

FIG. 3. Representative stress–strain curves for a model diblock copolymer lamellar structure in the weak segregation limit for two different m's ($m=9.3$ and $m=9.8$, corresponding, respectively, to $\chi N=12.070$ and $\chi N=12.108$). Other parameters are $N=1000$, $a=7.5$ Å, $v=113$ Å^3, and $T=350$ K. The + represents the quasithermodynamic melting point, and the × represents the limit of mechanical stability. The slope discontinuity at a very small, positive strain, is similar to that shown in Fig. 2(b), and is not shown here.

$$\frac{d\sigma}{d\epsilon}>0. \tag{3.32}$$

The vanishing of $d\sigma/d\epsilon$ thus defines the limit of mechanical stability. The strain at which this instability sets in can be found to be

$$\epsilon_{\rm ME}=\frac{1}{2s^{1/2}q_0^2}\left\{\frac{1}{2}\left(\frac{9\mu_R^2}{16\omega_R}-\tau_R\right)+\frac{1}{2}\left[\left(\frac{9\mu_R^2}{16\omega_R}-\tau_R\right)^2+\tau_R\left(\frac{3\mu_R^2}{4\omega_R}-\tau_R\right)\right]^{1/2}\right\}^{1/2}$$
$$=\frac{1}{2s^{1/2}q_0^2}(d\lambda)^{1/3}v^{1/3}a^{-1}N^{-1/6}\left\{\frac{1}{2}\tilde{\epsilon}_{\rm QT}^2(m)+\frac{1}{2}\left[\tilde{\epsilon}_{\rm QT}^4(m)+m^{-2/3}\tilde{\epsilon}_{\rm SP}^2(m)\right]^{1/2}\right\}^{1/2}. \tag{3.33}$$

For the weakly first-order transition described by the free energy Eq. (3.4), we can show that $\epsilon_{\rm QT}<\epsilon_{\rm ME}<\epsilon_{\rm SP}$. Note that all these three critical strains scale with the degree of polymerization as $\sim N^{-1/6}$ (for fixed m). Thus the dimensional critical stresses will scale as $\sigma\sim\epsilon A^2/N^{3/2}\sim N^{-3/2}$ for a given m. The lower left portion of Fig. 3 shows two representative stress–strain curves for two different m's, $m=9.3$ and $m=9.8$, corresponding, respectively, to $\chi N=12.070$ and $\chi N=12.108$ for some model diblock copolymer of polymerization degree $N=1000$. The molecular parameters are $a=7.5$ Å and $v=113$ Å^3. For these parameters, the critical χN is 12.067. The curves terminate at the spinodal for fixed strains; locations of the quasithermodynamic transition and the mechanical instability are indicated. In a stress experiment, the portion after the mechanical instability will not be reachable.

The difference between the spinodal for a controlled-strain experiment and the mechanical instability for a controlled-stress experiment becomes most pronounced for a hypothetical second-order transition described by the Landau free energy of Leibler, Eq. (3.3). In this case, the Gibbs free energy density is

$$g=(\tau+4sq_0^4\epsilon^2)A^2+(1/4)\mu A^4-\sigma(1+\epsilon) \tag{3.34}$$

with $\mu>0$. The order parameter for $\tau<0$ is obtained from $\partial g/\partial A=0$ which yields

$$A^2=(2/\mu)(|\tau|-4sq_0^4\epsilon^2) \tag{3.35}$$

and the stress–strain relation is given by

$$\sigma=8sq_0^4\epsilon A^2=(16/\mu)|\tau|sq_0^4\epsilon-(64/\mu)s^2q_0^8\epsilon^3. \tag{3.36}$$

In a strain experiment, the limit of metastability coincides with the quasithermodynamic transition; both take place when A decreases to zero. From this, we find

$$\epsilon_{\rm QT}=\epsilon_{\rm SP}=\frac{|\tau|^{1/2}}{2s^{1/2}q_0^2}. \tag{3.37}$$

On the other hand, the mechanical instability $d\sigma/d\epsilon=0$ sets in at

$$\epsilon_{\rm ME}=\frac{|\tau|^{1/2}}{2\sqrt{3}s^{1/2}q_0^2}. \tag{3.38}$$

Clearly, $\epsilon_{\rm ME}<\epsilon_{\rm QT}=\epsilon_{\rm SP}$. Furthermore, even though the equilibrium transition is second-order, occurring at $A^2=0$, the mechanical instability occurs at a finite value of the order parameter $A^2=4|\tau|/\mu=(2/3)A_0^2$, where A_0 is the value of the order parameter in the absence of stress or strain.

C. Tension

Tensile strain induces both a change in the amplitude of the composition wave and a spatial variation of its phase. For a given strain, the state of the system is obtained by minimizing the free energy Eq. (3.16) with respect to both A and $u(z;\mathbf{r}_\perp)$. We first minimize the free energy with respect to u while keeping A fixed. Because the explicitly strain-dependent terms in Eq. (3.15) are identical in form to Eq. (2.13) and because the analysis in Sec. II C is performed for general B and K without reference to their magnitude or any special relationship which may exist between them, we can simply transcribe our results in that section to the current situation. The critical strain is given by Eq. (2.22a) and the wave vector by Eq. (2.22b), with now $\Lambda=1/2q_0=D_0/4\pi$ in both equations. The undulation takes the form of a square-lattice wave, with the amplitude u_0 given by Eq. (2.26). The explicitly strain-dependent term of the free energy is simply

$$4A^2sq_0^4[\epsilon^2-\tfrac{3}{15}(\epsilon-\epsilon_c)^2\Theta(\epsilon-\epsilon_c)], \tag{3.39}$$

where we have inserted the step function [$\Theta(x)=1$ for $x>0$ and 0 otherwise] to have a single expression for both precritical and postcritical-strain states. The total free energy per unit volume thus becomes

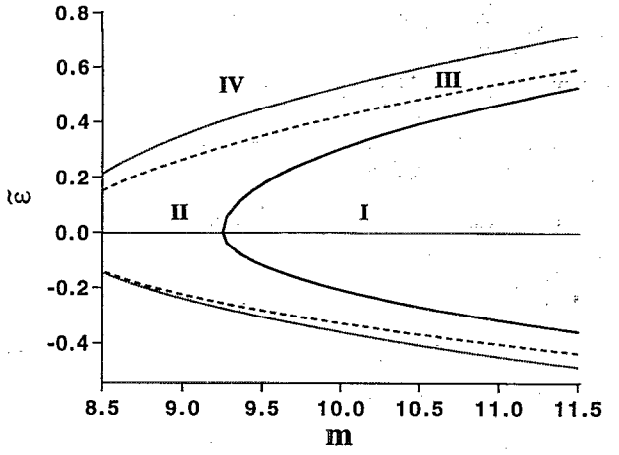

FIG. 4. Phase diagram in the scaled strain $\tilde{\epsilon}$ [cf. Eq. (3.42)] and the variable m [cf. Eq. (3.8a)]. The solid curve represents the quasithermodynamic melting line (QT), the dashed curve represents the mechanical instability (ME), and the dotted line represents the spinodal of the lamellar phase under controlled-strain conditions (SP). Regions I, II, and III correspond to lamellar states that are stable, thermodynamically unstable, and mechanically unstable, respectively, and region IV corresponds to the disordered states. In a stress-controlled experiment, the regions outside the line of mechanical instability is inaccessible.

$$f(A,\epsilon)=f_0(A)+4A^2sq_0^4[\epsilon^2-\tfrac{8}{15}(\epsilon-\epsilon_c)^2\Theta(\epsilon-\epsilon_c)]. \tag{3.40}$$

Unless the system is already very close to the equilibrium melting transition, the strains at which various melting instabilities take place are usually much larger than the critical strain ϵ_c for undulation, the latter being inversely proportional to the size of the system in the z direction. Therefore, in most cases, we expect that the system will first buckle before it melts. For very small ϵ_c, we can approximate Eq. (3.40) by

$$f(A,\epsilon)=f_0(A)+(28/15)A^2sq_0^4\epsilon^2\Theta(\epsilon) \tag{3.41}$$

and the analysis to obtain the strains for various melting instabilities under tension then proceeds exactly as that under compression, with a simple reduction of the coefficient of the ϵ^2 term to 7/15 of its value for the case of compression. This also means that the linear tensile modulus is 7/15 of the linear compressional modulus.

The full stress–strain curve, including the compression part, are shown in Fig. 3, with the various instabilities indicated. It can be seen that buckling moves the various strain-induced melting instabilities to larger strain and smaller stress in tension than in compression.

Because the various melting strains scale as $\epsilon\sim(1/2q_0^2)s^{-1/2}(d\lambda)^{1/3}v^{1/3}a^{-1}N^{-1/6}$ for a given m [cf. Eqs. (3.22), (3.23), (3.25), and (3.26)], it is natural to define a scaled strain

$$\tilde{\epsilon}=2s^{1/2}q_0^2(d\lambda)^{-1/3}v^{-1/3}aN^{1/6}\epsilon. \tag{3.42}$$

Then, we can construct a master phase diagram in terms of $\tilde{\epsilon}$ and m. The result is shown in Fig. 4. The full line represents the quasithermodynamic (QT) melting, the dashed line represents the limit of mechanical stability (ME), and the dotted line represents the spinodal (SP) under controlled strain conditions. An interesting feature of this phase diagram is the asymmetry between positive (tensile) and negative (compressional) strains, due to the layer undulation instability prior to the melting transitions under tension. Another feature is that the ME and SP lines become identical as we approach the spinodal point of the strain-free state ($m_s=8.2129$, not shown in the figure), while for large m (large χN), the ME line approaches the QT line. This last feature should be independent of the assumptions made in the current study, although quantitative predictions become poorer as χN increases further beyond the disorder–order transition.

IV. SUMMARY AND DISCUSSION

Although diblock copolymers are flexible molecules and lack the conspicuous orientation associated with the molecular axis in smectic liquid crystals of rigid molecules, the lamellar phase of diblock copolymers behave in many respects as smectics. Like the smectics, and probably more so than usual smectics because of the longer relaxation time in the polymer case, the diblock copolymer lamellar phase is capable of supporting quasistatic anisotropic stresses. In this paper, we have studied the thermodynamic and mechanical properties of the lamellar phase of diblock copolymers under uniaxial strains or stresses, in both the weak segregation limit and the strong segregation limit. Figures 2, 3, and 4, can be considered as representing the main results of our study.

One of the main predicitons of our theory is the asymmetry between the tensile and compressional parts of the stress–strain curve for both WSL and SSL, stemming from the layer undulation under tension, which occurs for very small strains. Using nonlinear continuum descriptions derived in this paper, we show that the apparent tensile modulus is 7/15 of the compressional modulus. Another prediction concerns the various strain-induced melting transitions in the WSL near the equilibrium order–disorder transition temperature. In particular, we show that in a stress-controlled rather than strain-controlled experiment, the mechanical instability (whose origin is nevertheless thermodynamic) is the relevant spinodal and always precedes the spinodal predicted by Amundson and Helfand.[11] The difference between these two spinodals become larger as χN is increased further beyond the order–disorder transition, and is most pronounced if the transition is a second-order one described by the Landau free energy of Leibler. The latter finding can also be regarded as yet another major difference between the mean-field theory and the fluctuation-renormalized theory. Under tensile stresses, we show that in most experimental situations melting happens after the layer undulation instability, and due to the reduction in the modulus following this instability, larger strains are required to induce melting of the lamellar structure.

What happens beyond the various melting strains? Our quasiequilibrium theory does not furnish an answer to this question. For strain-controlled situations, it is very likely that after melting into the isotropic phase, the system reorganizes into the lamellar structure with the equilibrium

layer spacing. However, the new lamellar structure is expected to be laden with defects, as the postmelting sample should behave like a system cooled into the ordered state from the disordered state, trapping in defects during the nucleation process. Hence the new lamellar sample is expected to be a poly-domain structure rather than a single-domain one. In a stress-controlled experiment, once the lamellae melt into the disordered phase it can no longer support a static anisotropic stress, and the system should begin to flow in an elongational pattern; the situation is similar to stress-induced melting of atomic solids at high temperatures.[34] Full dynamic considerations are then necessary to study this postmelting state.

Apart from the direct predictions we have made in this paper concerning the stress–strain relation and the various types of strain (stress) induced melting, our study should be relevant in understanding the defect structures in diblock copolymer mesophases. The interactions and spatial correlations among various types of defects are determined largely by the elastic, mechanical force balances. Thus understanding the mechanical behavior of single-domain structures provides the essential first steps for studying defects when single-domains with different orientations are put together. In particular, the nonlinear continuum free energy functionals Eqs. (2.12) and (3.15), should provide a framework for studying the structure around a defect where the deformations can be large. Our study should also be relevant in understanding the mechanism for flow-induced alignment of diblock copolymer microstructures which is a topic of intensive current interest.[5,35,36] One possible mechanism involves the melting of domains whose orientations are not favored by the flow directions. Clearly this melting is induced by local anisotropic stress concentration. Thus understanding of the quasistatic situations provides the basis for better understanding of such dynamic situations.

ACKNOWLEDGMENTS

The author wishes to thank J. A. Kornfield for a critical reading of the manuscript and helpful comments. This research was supported in part by a Fellowship from The Institute for Advanced Studies, The Hebrew University of Jerusalem, where the work began. Acknowledgement is also made to the Donors of The Petroleum Research Fund, administered by the American Chemical Society, for additional support.

[1] See, F. S. Bates and G. H. Fredrickson, Annu. Rev. Phys. Chem. **41**, 525 (1990), and references therein.
[2] A. Keller, E. Pedemonte, and F. M. Willmouth, Kolloid Z. Z. Polym. **238**, 25 (1970); Nature **225**, 538 (1970).
[3] G. Hadziioannou, A. Mathis, and A. Skoulios, Colloid Polym. Sci. **257**, 136 (1979); G. Hadziioannou and A. Skoulios, Makromol. Chem. Rapid Commun. **1**, 693 (1980); G. Hadziioannou, C. Picot, A. Skoulios, M.-L. Ionesku, A. Mathis, R. Duplessix, Y. Gallot, and J.-P. Lingelser, Macromolecules **15**, 263 (1982).
[4] F. A. Morrison, G. I. Bourvellec, and H. H. Winter, J. Appl. Polym. Sci. **33**, 1585 (1987).
[5] K. I. Winey, S. S. Patel, R. G. Larson, and H. Watanabe, Macromolecules **26**, 2542 (1993).
[6] T. A. Witten, L. Leibler, and P. A. Pincus, Macromolecules **23**, 824 (1990).
[7] P.-G. de Gennes, *The Physics of Liquid Crystals* (Clarendon, Oxford, 1974).
[8] J. M. Delrieu, J. Chem. Phys. **60**, 1081 (1974).
[9] M. Delaye, P. Ribotta, and G. Durand, Phys. Lett. A **44**, 139 (1973).
[10] N. A. Clark and R. B. Meyer, Appl. Phys. Lett. **22**, 493 (1973).
[11] K. Amundson and E. Helfand, Macromolecules **26**, 1324 (1993).
[12] E. Helfand and Z. R. Wasserman, Macromolecules **5**, 960 (1978); also in *Developments in Block Copolymers*, edited by I. Goodman (Applied Science, London, 1982), Vol. 1.
[13] T. Hashimoto, M. Shibayama, and H. Kawai, Macromolecules **13**, 1237 (1980); T. Hashimoto, M. Fujimura, and H. Kawai, *ibid.* **13**, 1660 (1980).
[14] A. N. Semenov, Sov. Phys. JETP **61**, 733 (1985).
[15] T. Ohta and K. Kawasaki, Macromolecules **19**, 2621 (1986); K. Kawasaki, T. Ohta, and M. Kohrogui, *ibid.* **21**, 2972 (1988).
[16] L. Leibler, Macromolecules **13**, 1602 (1980).
[17] J. Melenkevitz and M. Muthukumar, Macromolecules **24**, 4199 (1991).
[18] K. Kawasaki and T. Kawakatsu, Macromolecules **23**, 4006 (1990).
[19] K. Kawasaki and T. Ohta, Physica A **139**, 223 (1986).
[20] S. T. Milner and T. A. Witten, J. Phys. (Paris) **49**, 1951 (1988).
[21] Z.-G. Wang and S. A. Safran, J. Phys. (Paris) **51**, 185 (1990); J. Chem. Phys. **94**, 679 (1991).
[22] S. P. Gido and E. L. Thomas, Macromolecules (in press).
[23] M. S. Turner and J.-F. Joanny, Macromolecules **25**, 6681 (1992).
[24] The interfacial tension γ is related to the Flory–Huggins parameter χ as $\gamma \sim \chi^{1/2} a v^{-1}$. However, the precise relationship depends on the particular free energy functionals used in obtaining γ; see H. Tang and K. F. Freed, Chem. Phys. **94**, 6307 (1991).
[25] M. M. Kozlov and M. Winterhalter, J. Phys. II France **1**, 1077 (1991).
[26] These parameters do not correspond to any particular sample, but are given as estimates for typical diblock copolymers. The estimates on a and v are based on poly(ethylene–propylene)–poly(ethylethylene) (PEP–PEE) [from F. S. Bates, J. H. Rosedale, and G. H. Fredrickson, J. Chem. Phys. **92**, 6255 (1990)], while the estimate for γ is based on polystyrene-hygrogenated polybutadiene [from T. A. Witten, S. T. Milner, and Z.-G. Wang, in *Multiphase Macromolecular Systems*, edited by W. W. Culbertson (Plenum, New York, 1989)].
[27] R. L. B. Selinger, Z.-G. Wang, and W. M. Gelbart, J. Chem. Phys. **95**, 9128 (1991).
[28] Z.-G. Wang (unpublished results).
[29] S. A. Brazovskii, Sov. Phys. JETP **41**, 85 (1975).
[30] G. H. Fredrickson and E. Helfand, J. Chem. Phys. **87**, 697 (1987).
[31] G. H. Fredrickson and K. Binder, J. Chem. Phys. **91**, 7265 (1989).
[32] The wave vector renormalization enters at the two loop order; see Y. Levin, C. J. Mundy, and K. A. Dawson, Phys. Rev. A **45**, 7309 (1992).
[33] D. C. Morse and S. T. Milner, Phys. Rev. E **47**, 1119 (1993).
[34] R. L. B. Selinger, R. M. Lynden-Bell, and W. M. Gelbart, J. Chem. Phys. **98**, 9808 (1993).
[35] K. Koppi, M. Tirrell, F. S. Bates, K. Almdal, and R. H. Colby, J. Phys. II France **2**, 1941 (1992).
[36] R. M. Kannan and J. A. Kornfield, Macromolecules (submitted).